BULLETIN OF THE POLISH ACADEMY OF SCIENCES
TECHNICAL SCIENCES, Vol. 68, No. 3, 2020
DOI: 10.24425/bpasts.2020.133385

Experimental research on separation efficiency of aerosol particles in vortex tube separators with electric field

T. DZIUBAK*

Military University of Technology, 2 Gen. Sylwestra Kaliskiego St., 00-908 Warsaw, Poland

Abstract. A comparative analysis of filtration performance of tangential and axial inlet reverse-flow cyclone separators and vortex tube separators is presented. The study showed that vortex tube separators are characterized by a quality factor q several time higher than tangential inlet reverse-flow cyclone separators. The cyclone separators yield low separation efficiency and low filtration performance at low air flow rates at low air volumes aspired by the engine at low speed. One of the well-known and not commonly used methods to improve separation efficiency is to apply electric field. An original design of a vortex tube separator with insulators generating electric field in the area of aerosol flow is presented. High voltage was applied to the cyclone separator housing and its swirl vane. A special method and test conditions were developed for cyclone separators with electric field. Separation efficiency, filtration performance and pressure drop across the cyclone separator in two different variants were determined. The tests were carried out at five inlet velocity of cyclones $\upsilon_0 = 1.75$; 3.5; 7.0; 10.5; 14 m/s at an extraction rate of $m_0 = 10\%$, and at an average dust concentration in the inlet air of $s = 1$ g/m^3. Using the electric field in the area of a swirling aerosol stream resulted in an increase (over 12% – $\varphi_c = 96.3\%$) in separation efficiency at inlet velocity of cyclone ranging from 1.75 to 3.5 m/s. An increase in separation efficiency at other inlet velocity of cyclone is minor and does not exceed 3–4%.

Key words: vortex tube separator, electric field, separation efficiency and filtration performance, pressure drop across the cyclone separator, experimental research.

1. Introduction

Cyclone separators are separation devices that use the principle of inertia (centrifugal-force field) to remove particulate matter from liquids. Simple and compact design, resistance to high temperature and pressure, simple maintenance and the ability to separate a large amount of particulate matter from the air stream made the cyclone separator a commonly used device in industrial applications [1] and in filtration processes of intake air in turbine helicopter engines, including: Mi-17/Mi-8MT [2], Ch-47 Chinook [3], AS332/EC725 Super Puma [4]. Cyclone separators are also used as the first filtration stage in reciprocating internal combustion engines operating in high-dust concentration areas (military and special vehicles), where the dust concentration in the air exceeds 1 g/m^3 [5–9].

The use of cyclone separators in filtration of intake air in reciprocating internal combustion engines is limited by low separation efficiency of small particles and constantly changing and pulsating air flow in the air intake system, which may affect cyclone separator operation. Cyclone separators are very effective at high air flow rates, usually over 10 m/s. At idle speed, the air stream at the engine inlet is low, and the cyclone separator may be inefficient.

The cyclone separators used in motor vehicles at rated working conditions are characterized by separation efficiency of up to 96%, and filtration performance of up to $d_{zmax} < 15$–35 μm [10–15]. New modifications of the design to improve the separation efficiency of the efficiency of the aerosol particles and to reduce the pressure drop in cyclone separators are being investigated.

Studies show that the cyclone separator efficiency can be improved by applying electric field to the aerosol particles. Electrostatic aerosol filtration technique is commonly used in power industry, heat engineering, metallurgy for filtering flue gases, as well as in chemical, cement and paper industry [16–18]. The electric field is also used to produce polymer nanofibers by electrospining [19–22]. Nanofibers of very small diameters (around 50÷800 nm) are used, among others, in automotive technology as the filter material of the intake air of internal combustion engines [8].

The electrostatic filtering devices use electrostatic precipitators in treatment of gases containing a significant amount of dust as a result of fuel combustion in the power boilers. At a nominal gas flow rate (approx. 1 m/s) and at 80 to 135 kV, the separation efficiency of the electrostatic precipitator may reach up to 99.96% [17]. Since electrostatic precipitators are large devices designed to treat large volumes of aerosols, they cannot be used at low air flow rates, usually observed in the intake air systems of motor vehicles. Preliminary filtration of the intake air of special vehicles usually relies on low-diameter ($D = 35$ to 40 mm) cyclone units.

The research presented in the article was aimed at improving return cyclone with a tangential inlet efficiency by applying a high voltage electric field in the area of a rotating aerosol. These were cyclones with mainly industrial applications, intended for waste gases filtration coming from technological processes, whose cylindrical part diameter D and height H sig-

*e-mail: tadeusz.dziubak@wat.edu.pl

Manuscript submitted 2019-12-05, revised 2020-01-20, initially accepted for publication 2020-02-12, published in June 2020

nificantly exceed cyclone main dimensions used in vehicles air filters. Available cyclone-electric field test results do not include vortex tube separators with axial inlet, which are commonly used in modern intake air filtration systems for truck engines, working machines, agricultural tractors and helicopters, as the first stage of air filtration.

Increasing cyclone filtration efficiency and accuracy means reducing the mass of dust directed to the second stage of filtration – a paper insert. Due to the limited mass absorption of the filter paper, filter operating time is limited by permissible pressure drop value Δp_{dop}. Therefore, the actions taken in this work and aimed at testing vortex tube separators in terms of improving filtration efficiency and accuracy, and reducing pressure drop are justified.

2. Theoretical basics

Due to the principle of operation, cyclone separators can be classified as reverse-flow cyclone separators (Fig. 1a, Fig. 1b) in which the aerosol particles change the flow direction by 180° and vortex tube separators (Fig. 1) in which the aerosol particles do not change the flow direction. The gas stream can be set in rotary motion as a result of tangential inflow to the cylindrical section of the cyclone separator (Fig. 1a) or as a result of flow through the fixed swirl vane with helical blades (Fig. 1b, Fig. 1c).

Aerosol particle filtration in the cyclone separator, despite its simple design is a very complex process. It is mainly due to advanced gas motion which involves not only rotary motion (screw motion) but also two-directional reverse-flow motion and many auxiliary phenomena. Motion of the dust particles in cyclone separator is a relative motion in relation to the fixed device walls and the gas flowing inside the cyclone separator. The motion takes place in a gas flow rate field variable in space (and specific for each cyclone design), and thus is affected by the system of forces acting on each particle, variable in space. Additional factors include variable particle size distribution, density, shape and resulting variable inertial and aerodynamic forces. The particles collide with the cyclone separator walls and with each other causing the dust to coagulate.

Figure 2 shows the performance characteristics of tangential inlet reverse-flow cyclone separators (A, B), axial inlet reverse-flow cyclone separators (C) and vortex tube separators (E, F) determined at the same test stand, under the same test condition and using the same test dust.

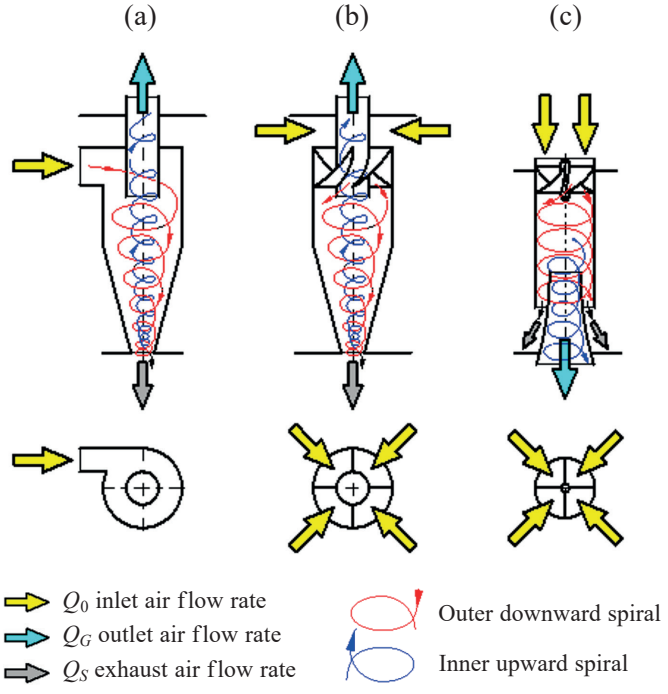

Fig. 1. Design of the cyclone separator used in motor vehicle air filters: a) tangential inlet reverse-flow cyclone separator, b) axial inlet reverse-flow cyclone separator, c) vortex tube separator

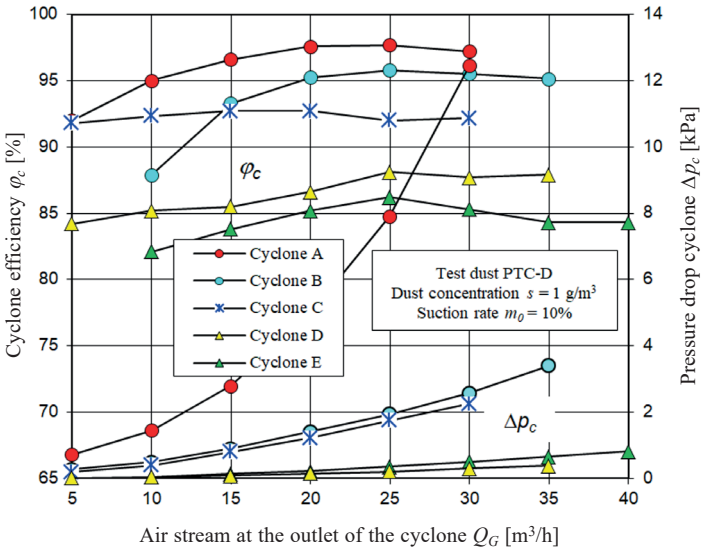

Fig. 2. Separation efficiency $\varphi_c = f(Q_G)$ and pressure drop $\Delta p_c = f(Q_G)$ of the tangential inlet reverse-flow cyclone separators (A, B, C) and vortex tube separators (D, E)

A comparative analysis shows that the tangential inlet reverse-flow cyclone separators (A, B) feature high separation efficiency and high pressure drop compared to other cyclone separators. The vortex tube separators (D, E) show 10% lower separation efficiency and significantly lower pressure drop. For the air flow rate of $Q_G = 35$ m³/h, pressure drop across the cyclone separator E is $\Delta p_c = 0.46$ kPa, and is several times higher at $\Delta p_c = 3.4$ kPa across the cyclone separator B. The filtration performance of the cyclone separators can be compared using a quality factor q determined using the following relationship [23, 24]:

$$q = \frac{-\ln(1-\varphi_0)}{\Delta p} \left[1/\text{kPa}\right] \tag{1}$$

where: φ_c – separation efficiency, Δp – pressure drop [kPa].

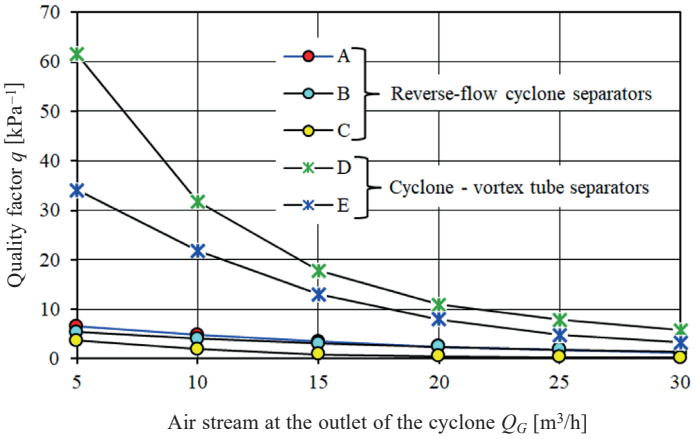

Fig. 3. The quality factor q for reverse-flow cyclone separators (A, B, C) and vortex tube separators (D, E)

Figure 3 shows that the quality factor q for vortex tube separators is several times higher than for tangential inlet reverse-flow cyclone separators. The quality factor q defined in this way optimizes the cyclone separator performance with regard to separation efficiency and pressure drop only. The factor does not allow for the filtration performance of the cyclone separator, which along with the pressure drop increases significantly with the increase in air flow rates.

Due to high separation efficiency, high filtration performance and low pressure drop, the cyclone separators should be able to operate within a limited air flow rate range resulting from the inlet velocity of cyclone υ_0.

This is the average speed at the cyclone inlet, which is defined by the relationship:

$$\upsilon_0 = \frac{Q_0}{A_0}\,[\mathrm{m/s}], \tag{2}$$

where: Q_0 – aerosol air flow rate at the cyclone separator inlet, A_0 – cross-sectional area of the inlet port at its most narrow section.

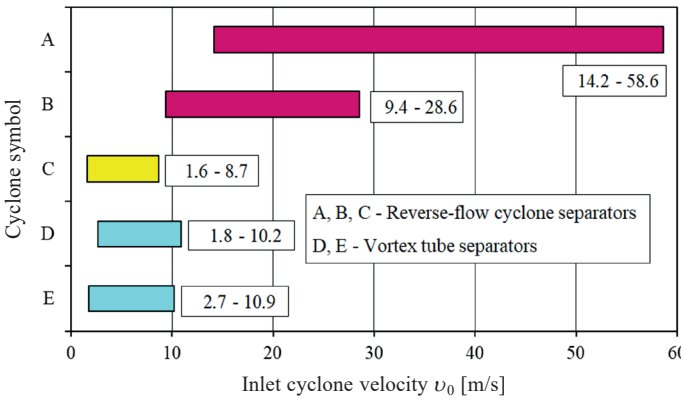

Fig. 4. The inlet velocity of cyclone υ_0 of cyclone separators used in the air filters of selected military vehicles: A, B – cyclone separators in the air filters of tracked vehicles; C, D, E – cyclone separators in the air filters of wheeled vehicles

For the tangential inlet reverse-flow cyclone separators, this range is $\upsilon_0 = 10$–25 m/s, and for the vortex tube separators it is $\upsilon_0 = 3$–10 m/s [7, 12, 14]. Figure 4 shows changes in the inlet velocity of cyclone υ_0 of the cyclone separators used in the air filters of selected military vehicle engines resulting from the air flow rate at the engine intake and the engine speed range of $n_{min} - n_N$.

Figure 5 shows the performance characteristics of the tangential inlet reverse-flow cyclone separator (tracked vehicle air

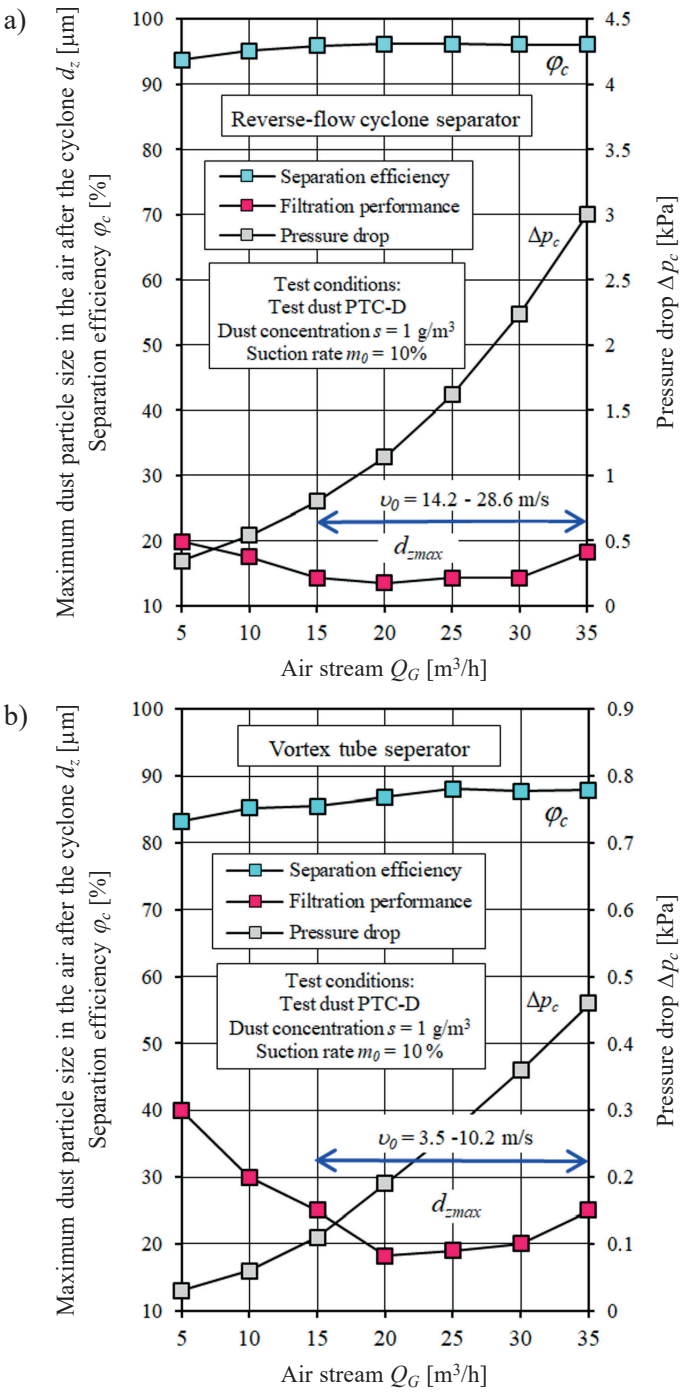

Fig. 5. Separation efficiency $\varphi_c = f(Q_G)$, filtration performance and pressure drop $\Delta p_c = f(Q_G)$ of cyclone separators: a) tangential inlet reverse-flow cyclone separator, b) vortex tube separator [7, 12]

filter) and the vortex tube separator (wheeled vehicle air filter) within the same air flow rate range Q_G. Conventional range resulting from the maximum separation efficiency and the minimum dust particle concentration in the tested cyclone separators is: $\upsilon_0 = 14.2–28.6$ m/s and $\upsilon_0 = 3.5–10.2$ m/s, respectively. Figure 5 shows that the low separation efficiency and low filtration performance are observed for the cyclone separators at low air flow rates, resulting from low inlet air flow rates at low engine speed, e.g. idle gear or low load. One of the methods to increase the separation efficiency of cyclone separators at low air flow rates is to use the electric field.

The main component of the vortex tube separator is a swirl vane integrated in the front section of a cylindrical body. The swirl vane usually has four helical blades (guide vanes). The aerosol inlet to the body may be shaped by a lemniscate. At a specific distance l_s from the swirl vane, a conical outlet tube is installed inside the body. The cross-sectional area of the outlet tube A_w increases in the direction of the air outlet. An outer wall of the outlet line and an inner wall of the cylindrical section of the body form a separation chamber at a section a (Fig. 6).

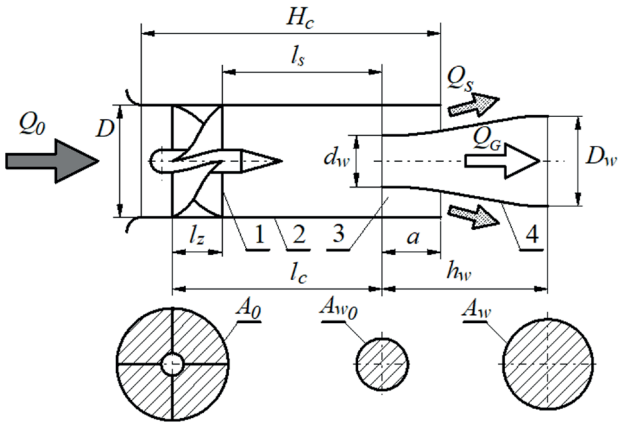

Fig. 6. Main components and dimensions of the vortex tube separator: 1 – swirl vane, 2 – cylindrical section, 3 – dust separation chamber, 4 – outlet tube, Q_0 – cyclone inlet air flow rate, Q_G – outlet air flow rate, Q_s – exhaust air flow rate, H_c – height of the cylindrical section, l_s – distance between the swirl vane and the separation chamber, D – swirl vane diameter, l_z – swirl vane length, d_w – outlet tube inlet diameter, D_w – outlet tube outlet diameter, a – separation chamber length, l_c – cyclone working section length, h_w – outlet tube length

The guide vanes, due to the required tolerances and precision, are the most complex part of the cyclone separator. The outer diameter of the swirl vane corresponds to the outer diameter D of the cyclone.

In the modern intake air filtration systems used in trucks, heavy machinery, tractors and helicopters, the vortex tube separators are commonly used as the first filtration stage. Thus, the studies on vortex tube separators to improve the separation efficiency and filtration performance and to reduce the pressure drop are well-grounded. A large number of parameters affecting the efficiency of cyclone separators and high processing power of advanced computers allowed CFD (computational fluid dynamics) software to be applied to eliminate time-consuming and expensive experimental tests at the design stage. Many studies presenting the models to separate the aerosol particles in the tangential inlet reverse-flow cyclone separators are available in the literature: [25–30], however, numerical analyses of the aerosol filtration in vortex tube separators are rare [23, 31–34].

The most reliable research method, despite high costs and availability of many professional numerical computer applications are still the experimental tests on tangential inlet reverse-flow cyclone separators [11, 12, 14, 35–40] and vortex tube separators [14, 15, 41, 42].

Using the electric field to improve the efficiency of cyclone separators resulted in a new design – an electro-cyclone separator. The electro-cyclone separator is an electro-inertial aerosol filter based on the inertial separator, where the particles are subject to inertial force and are separated from the air stream, whereas high voltage attracts the particles to specific surfaces. Both techniques are commonly used in the industry; however, using both in a single device is limited.

According to [43–45], the electro-cyclone separator is a type of an electrostatic precipitator (ESP) in which the aerosol flow is rotational and translational. Many authors claim that the electro-cyclone separator is a combination of the cyclone separator and the electrostatic precipitator [46–48] and combine the inertial and electrostatic separation based on the conventional cyclone separator with an auxiliary high-voltage electrostatic field. The studies on electro-cyclone separators have begun over 40 years ago [43]. Various designs of electro-cyclone separators often involving a cyclone separator in form of a tube with a discharge electrode placed inside the cyclone separator [46, 49–51].

There are several benefits to using electro-cyclone separators, including simple design and low operating costs. The separators are commonly used in the industry and have a potential for use as advanced dust removal devices. A rational selection of the cyclone separator and the corona electrode location allows to achieve an optimum distribution of flow rates in the cyclone separator to improve the particle separation using inertial force by reducing the resistance in the electro-cyclone separator [44, 45, 48]. Various electro-cyclone separator designs are available featuring a corona electrode installed in the cyclone separator [52]. The number and the position of the corona electrodes in the cyclone separator affect the effect of electrostatic field [52]. Studies [53–55] discuss electro-cyclone separators, in which high voltage is supplied to the discharge electrode installed in the cyclone separator axis to generate corona discharge ions and electrostatic force. Accumulation of charges on fine airborne silica particles in the electro-cyclone separator results in a significant increase in its separation efficiency. Direct relationship between the separation efficiency and the charging voltage was also observed, where the overall separation efficiency increased from 2.7% to approx. 72% due to the increase in charging voltage from 0 kV to 18 kV [56].

In article [50, 53], a reverse electrostatic cyclone with a tangential inlet with a diameter of $D = 206$ mm was designed for

removing ash from the exhaust gases from a power plant. The electrodes forming the crown were placed in the active zone of the cyclone with a length of 1250 mm. The corona forming system consists of three rods with needles positioned every 40 mm. High filtration efficiency (about 99%) was obtained in the cyclone inlet speed in range of 10–14 m/s for dust grains below 40 μm and voltage of 17 kV.

In [52], for different air flows $Q = 15{,}75$, 28,75 and 44,26 m^3/min, an electrocyclone with a diameter of $D = 220$ mm with 1 m electrode and a diameter of 25 mm located centrally in the axis of the cyclone was examined and voltage of 25 kV was applied. At low air flow, electrocyclone efficiency is much greater than the one in cyclone. As the flow velocity increases, influence of electric field decreases. At maximum flow rate, the efficiency of the electrocyclone is similar to the one in cyclone.

Boericke et al. [57] used an electrocyclone with a diameter of $D = 457$ mm to test the gas filtration efficiency, containing fly ash from coal. Four types of electrodes were used, which were centrally hanged inside the cyclone outlet channel. The results showed that the electrocyclone filtration efficiency at applied voltages (0, 60, 70 and 75 kV) was much higher than the efficiency of the cyclone, but only at lower flow rates, which was due to particles longer residence time in the cyclone electric field. As expected, the improvement is relatively small at high flow rates at which performance is dominated by inertial (centrifugal) effects.

The number and location of corona electrodes in the cyclone affects the strengthening effects of electrostatic field. Dietz [53] strengthened the cyclone separator by putting an electric force, and Plucinski et al. [54] and Gradon et al. [58] applied high voltage to the vortex detector instead, to the central wire for charging particles. Plucinski et al [54] who were examining the return cyclone with a tangential inlet with a diameter of $D = 40$ mm determined that the electric field has the most significant effect for small particles and at low gas speed. A qualitative experimental verification of this effect was also carried out for silica particles with a diameter in the range of 0.5 to 5 μm at 8 kV and an inlet speed $\upsilon_0 = 2$–12 m/s. The results showed that the efficiency of the cyclone decreased with increasing gas inlet speed into the cyclone.

The model developed by Dietz [53] includes two important assumptions: firstly, it was assumed that the electrode structure does not affect the fluid vortex mechanics, the second – all particles reaching the wall are collected by it. The results showed that at lower fluid flow rates, the impact of electrostatic forces is decisive – a significant improvement in filtration efficiency has been achieved.

The motion of the dust particle in the cyclone separator is usually considered as a motion in a plane perpendicular to the cyclone separator axis. Based on this assumption, the dust particle in the cyclone separator with electric field is affected by the inertial force F_B, aerodynamic resistance of the medium F_R and electrostatic force F_E (Fig. 7).

The dust particles move at the trajectory determined by the interrelations between those forces. The forces depend on dimension, shape and material of the particle and the medium type. A vortex motion of the aerosol results in an inertial force

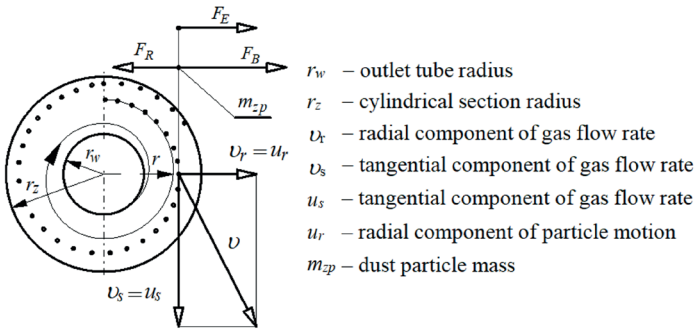

Fig. 7. Forces acting inside the cyclone separator with electric field: F_E – electrostatic force, F_B – centrifugal force, F_R – drag force

F_B acting on the dust particle with a mass m_{zp} at a distance r from the axis of rotation [59]:

$$F_B = \frac{m_{zp} \cdot u_s^2}{r}, \tag{3}$$

where: u_s – tangential component of particle flow rate equal to the tangential component of gas flow rate υ_S at the same point.

In the same direction as the inertial force F_B, an electrostatic force F_E in accordance with [45] can be observed:

$$F_E = q_{es} E, \tag{4}$$

where: q_{es} – particle charge, E – local electric field strength [V/m].

The forces result in the particle motion in the direction of the cyclone separator wall at a flow rate u_r. The motion is counteracted by the resisting force of the medium F_R determined from the following relationship [59]:

$$F_R = \lambda \cdot A_p \frac{u_r^2}{2} \rho_g, \tag{5}$$

where: A_p – particle projection surface area in the motion direction, u_r – radial component of particle motion, ρ_g – gas density, λ – frictional resistance coefficient:

$$\lambda = f(\psi_k, R_e), \tag{6}$$

where: Ψ_k – particle shape factor, R_e – Reynolds number.

In accordance with the Newton's law for the radial component of motion u_r, at resistance directed inside (axis) of the cyclone separator, the equation of motion for the particle is [45]:

$$m_{zp} \cdot \frac{du_r}{dt} = \frac{m_{zp} \cdot u_s^2}{r} + q_{es} E - \lambda \cdot A_p \cdot \frac{u_r^2}{2} \cdot \rho_g. \tag{7}$$

The dust particles with the diameter lower than a specific dimension d_{zg} defined as a limit diameter of the particle for which $F_B + F_E < F_R$ will enter the cyclone separator and will be captured by the internal vortex in the direction of the outlet

tube of the cyclone separator. The separation efficiency of those particles in the cyclone separator is 0%. The dust particles with diameter over d_{zg}, for which $F_B + F_E > F_R$ will move on a spiral and will be pushed to the cyclone separator walls and will be separated with 100% efficiency. The particles with a diameter of d_{zg}, for which $F_B + F_E = F_R$ will theoretically travel around the circle with a radius r. In practice, the dust particles in the cyclone separator will move within a gas flow rate field variable in space under the system of forces acting on each individual particle, also variable in space. The dust particles will have a variable and irregular shape and resulting differences in ratio of inertial and aerodynamic forces, and the particles will collide with the cyclone walls and with each other causing the dust to coagulate. Due to those factors, not all dust particles with a size over d_{zg} will be separated in the cyclone with 100% separation efficiency. Not all particles with the sizes smaller than d_{zg} will be captured in 100% by the internal air vortex in the direction of the outlet tube of the cyclone. The particles not meeting the condition $F_B + F_E = F_R$ will not move around a circle with a specific radius. Some particles will be separated in the cyclone, some will be captured by the internal vortex in the direction of the cyclone outlet. Dust particle size for which the separation efficiency is 50% is referred to as the limit particle diameter d_{zg} and is designated as d_{50}.

The effect of different conditions on the separation efficiency of the particles with a diameter exceeding 0.5 μm was tested in [52, 55, 60–62,] as part of the experimental tests and in [44, 45, 53, 54] as part of the numerical analyses. In electro-cyclone separators, high voltage is supplied to the discharge electrode or the swirl vane [53–55] installed in the axis of the cyclone separator to generate corona discharge ions and electrostatic force. The electric charges are accumulated on the particles entering the electro-cyclone separator, and the particles are discharged to the collecting wall through an electrostatic force combined with an inertial force [44, 45, 63]. The separation efficiency of the particles by the electro-cyclone separator increases with the residence time [52], voltage [61, 62], dust load [23, 62] and length of the discharge electrode and the collecting electrode [60, 61]. The separation efficiency of particles from 0.5 to 10 μm may reach up to 99%, as show in [61]. In the available literature, there are no experimental data on the separation efficiency of particles smaller than 0.5 μm in the electro-cyclone separators and no numerical models are available.

An electro-cyclone separator with a centrally installed discharge wire show in [61] was used to test the factors affecting the separation efficiency of particles from 0.5 to 10 μm by changing the operating conditions and parameters of the particle size. The discharge wires with different diameter and length were supplied with a voltage from 0 to 9 kV. Two types of swirl vane material was used: aluminium and acrylic. To evaluate the effect of the electrostatic force, swirl vanes with three different lengths: 25, 35 and 45 mm were used. The tests showed that an increase in voltage and reduction in wire diameter increases the separation efficiency of small particles, usually at low flow rates.

3. Purpose and subject of the study

The purpose of the tests was to evaluate the efficiency of the vortex tube separator with and without electric field. This purpose was achieved by determining the following performance characteristics of the cyclone:

- separation efficiency $\varphi_c = f(\upsilon_0)$;
- filtration performance $d_{zmax} = f(\upsilon_0)$;
- pressure drop $\Delta p_c = f(\upsilon_0)$.

The tested product was a prototype axial inlet vortex tube separator (designed and manufactured by Laserstar Sp. z o.o. Sp. k. Toruń) – Fig. 8 [64].

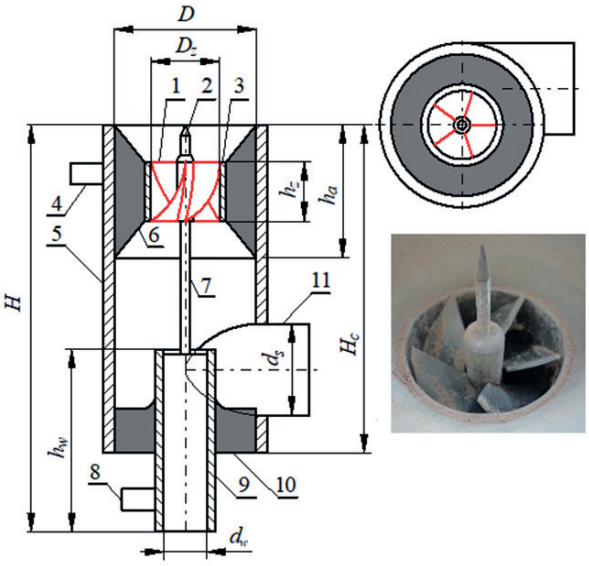

D – inside diameter of the cylindrical part
D_z – swirl diameter
H – total height of the cyclone
H_c – height of the cylindrical part
h_w – gas outlet pipe height
d_w – inside diameter of the outlet tube
h_z – swirl length
h_a – top insulator length
d_s – diameter of the dust extraction hose

D = 66 mm
D_z = 37 mm
H = 137 mm
H_c = 115 mm
d_w = 19 mm
h_z = 25 mm
h_a = 106 mm

Fig. 8. Vortex tube separator structural diagram that is the subject of exploratory research: 1 – swirl vane blades, 2 – negative electrode terminal, 3 – swirl vane external ring, 4 – high voltage terminal (ground), 5 – cylindrical section of the cyclone (housing-ground), 6 – top isolator, 7 – connecting pin, 8 – high voltage terminal (negative), 9 – cyclone outlet tube, 10 – bottom insulator, 11 – dust extraction pipe [64]

The air swirl in the cyclone separator is generated by a 5-blade swirl vane (S = 95 mm pitch) installed at the cyclone separator inlet between a centre pin and an external cylindrical ring. The centre pin of the swirl vane has a needle – a terminal of the negative electrode facing the inflow air. A set of swirl vane blades with the needle is connected with the filtered air outlet tube with a special pin. The components are made of steel and form a negative electrode. An insulating layer is positioned between the blades and the cylindrical cyclone housing made of steel. Similar insulating layer is located between the outlet tube

and the cyclone housing. The layers separate the negative electrode from the housing which in this case is a "ground" (Fig. 8).

The study aimed to determine the following performance characteristics: separation efficiency, filtration performance and pressure drop of the vortex tube separator with and without electric field for two cyclone separator variants – basic W1 and modified W2.

4. Test methods and conditions

The tests were carried out at four inlet velocity of cyclone $\upsilon_0 = 3.5$; 7.0; 10.5; 14 m/s (for W2 and $\upsilon_0 = 1.75$ m/s) at a dust extraction rate $m_0 = 10\%$ and at an average dust flow concentration in the inlet air $s = 1$ g/m^3. The inlet velocity of cyclone υ_0 are within the range observed in the vortex tube separators commonly used in the air filters of modern motor vehicles.

At the selected inlet velocity of cyclone υ_0 the main air flow rate Q_G and the dust extraction flow rate Q_S were calculated using the following relationship:

$$Q_G = 3600 \cdot \upsilon_0 \cdot A_0 \left[\mathrm{m^3/h}\right], \tag{8}$$

where: A_0 – cross-sectional area of the air inlet port with an inner diameter of $D_z = 37$ mm (outer diameter of the cyclone's swirl vane).

The air stream Q_S extracted from the cyclone is determined based on the following relationship:

$$Q_S = m_0 \cdot Q_G \left[\mathrm{m^3/h}\right], \tag{9}$$

where: m_0 – dust extraction rate from the cyclone separator (in commonly used inertial filters it is between 8 and 15%). Extraction rate of $m_0 = 10\%$ was used.

The tests were carried out on a specially designed test stand (Fig. 9) to determine basic performance characteristics of cyclone separators.

The main component of the test stand is the analysed vortex tube separator, arranged vertically and fixed to the laboratory workbench. The cyclone outlet line discharging the stream of filtered air and the extraction line discharging the separated dust are connected to the test stand components with insulating lines 9 and 12.

At a distance of $6d_w$ (where d_w – inner diameter of the measuring line – outlet tube), a liquid manometer (U-tube manometer) is connected downstream of the tested separator to measure static pressure drop Δh and to determine the pressure drop across the cyclone Δp_c.

An absolute filter no. 1 and an absolute filter no. 2 are installed downstream of the measuring line 12. The filters protect the rotameter used to measure the main air flow rate Q_G against dust and are also used as the measuring filters to determine the mass of dust m_{A1} and m_{A2} downstream of the cyclone separator. The absolute filter 16 protecting the rotameter (used to determine the extraction flow rate Q_S) is installed at the extraction line 8. The mass of dust m_D upstream of the cyclone separator and the mass of dust downstream of the cyclone separator m_{A1} and m_{A2} were determined using an analytical balance with a measuring range of 220 g and accuracy of 0.0001 g.

Using the particle counter at the test stand allows to determine the number and size of dust particles downstream of the

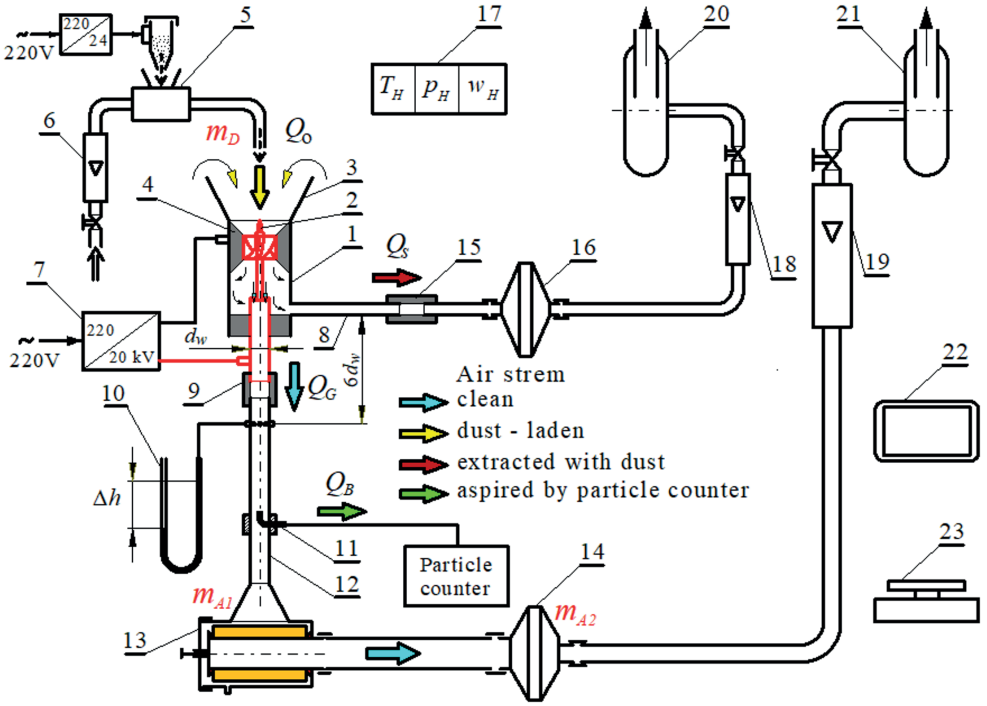

1 – tested cyclone,
2 – electrode,
3 – dust chamber,
4 – swirl vane isolator,
5 – dust dispenser,
6 – compressed air rotameter,
7 – high voltage power supply,
8 – extraction line,
9 – insulating fitting,
10 – U-type water manometer tube,
11 – particle counter measuring probe,
12 – outlet line (measuring line),
13 – absolute filter of the main line No 1,
14 – absolute filter of the main line No 2,
15 – insulating fitting,
16 – extraction line absolute filter,
17 – set for pressure, temperature and humidity measurement relative ambient air,
18 – extraction flow rate Q_s rotameter,
19 – main flow rate Q_G rotameter,
20 – extraction air flow rate Q_s fan,
21 – main air flow rate Q_G fan,
22 – computer for recording test results,
23 – analytical balance

Fig. 9. Test stand for the vortex tube separator with axial inlet with devices for generating electric field

cyclone separator. The probe samples the tested air flow rate Q_B – a sample of the air stream Q_G directed to a sensor. The sensor analyses the number N and size d_z of the dust particles. The voltage signal is send to the *Pamas*-2132 particle counter microchip. The device sensor counts the particles within the range of 0.7÷100 μm in 32 measuring intervals within the following range (d_{zmin} to d_{zmax}).

The main air flow rate Q_G, extraction air flow rate Q_S and compressed air flow rate Q_{SPR} upstream of the dust supply unit were determined based on the readouts from the float type rotameters (RIN type) and calibration curves. All rotameter shave an accuracy class of 2.5.

A high-voltage power supply 50 kV was used to generate the electric field. For W1 cyclone separator, voltage between $U_E = 16.5$ to 16.8 kV ($U_E = 18.5$ to 19 kV for W2 variant) was used. Higher voltages were not available due to a breakdown between the negative electrode and the ground (between the outlet line and the cyclone housing).

The tests were carried out in measuring cycles corresponding to the time t_p of uniform dust supply to the cyclone. During the measuring cycle, at $t_z = {}^1\!/_2 t_p$, a particle counter was activated to count the number and size of the dust particles in the air downstream of the cyclone separator.

PTC-D test dust, an equivalent of AC-fine test dust was used. The chemical composition and particle-size distribution of the test dust are shown in [17].

Nine (9) measuring cycles were carried out for each cyclone outlet flow rate υ_0 (a specific main air flow rate Q_G value). The following were determined after each measuring cycle j:

1. Pressure drop Δp_c across the cyclone separator as a static pressure drop at the outlet line in the distance of $6d_w$ from the face of the cyclone body (where d_w – inner diameter of the cyclone outlet line) based on the U-tube manometer readouts Δh_m [mm H_2O] in accordance with the following relationship:

$$\Delta p_c = \frac{\overline{\Delta} h_m}{1000} \cdot (\rho_m - \rho_H) \cdot g \,[\mathrm{Pa}], \tag{10}$$

where: $\overline{\Delta} h_m$ – average from nine measurements for a specific outlet flow rate υ_0, ρ_m – manometric liquid density $[\mathrm{kg/m^{-3}}]$, ρ_H – air density $[\mathrm{kg/m^{-3}}]$, g – gravitational acceleration $[\mathrm{m/s^2}]$.

2. Separation efficiency φ_c, as a quotient of mass of dust retained by the cyclone m_{zc} and supplied to the cyclone m_D (gravimetric method) in the measuring cycle with $t_p = 3$ min duration using the following relationship:

$$\varphi_c = \frac{m_{zc}}{m_D} \cdot 100\%, \tag{11}$$

where: m_{zc} – mass of dust retained (in time τ_p) by the cyclone, m_D – mass of dust supplied to the cyclone in time τ_p at the inlet air flow rate Q_0.

The mass of dust m_{zc} retained by the cyclone in the measuring cycle in τ_p was determined indirectly from the following relationship:

$$m_{zc} = m_D - (m_{A1} + m_{A2}) \,[\mathrm{g}], \tag{12}$$

where: m_{A1}, m_{A2} – mass of dust retained in time τ_p at the absolute filter No. 1 and No. 2.

3. Filtration performance as the largest dust particle size $d_{zj} = d_{zmax}$ in the air downstream of the filter.
4. Percentage share Up_i of the number of dust particles N_i from each measuring interval i ($d_{zimin} \div d_{zimax}$) in the total number of dust particles N in the air downstream of the cyclone (the number of dust particles from all measuring intervals) using the following relationship:

$$Up_i = \frac{N_i}{N} = \frac{N_i}{\sum_{i=1}^{32} N_i}. \tag{13}$$

Actual dust concentration in the cyclone inlet air during each measuring cycle was calculated after finishing the cycle using the following relationship:

$$S_j = \frac{m_{Dj}}{Q_{0j} \cdot t_{pom}} = \frac{m_{Dj}}{(Q_{Gj} + Q_{Sj}) \cdot t_{pom}}, \tag{14}$$

where: t_{pom} – time, in which the mass of dust m_{Dj} was supplied uniformly to the air stream Q_0 at the cyclone inlet.

After $j = 9$ measuring cycles for each flow rate υ_0 (air flow rate Q_G), average separation efficiency φ_c, pressure drop Δp_c and dust concentration s were calculated.

5. Vortex tube separator– variant W1 – test result analysis

Figures 10 and 11 show the test and calculation results for separation efficiency, filtration performance $\varphi_c = f(\upsilon_0)$ and flow characteristics $\Delta p_c = f(\upsilon_0)$ of the vortex tube separator (W1) with and without electric field.

With the increase in air flow rate Q_G and the inlet velocity of cyclone υ_0, a parabolic increase in pressure drop Δp_c across the tested cyclone separator can be observed (Fig. 10a). For the maximum inlet velocity of cyclone $\upsilon_0 = 14$ m/s ($Q_G = 50$ m^3/h) the pressure drop across the cyclone separator is $\Delta p_c = 2.3$ kPa. It is a significant value for this type of cyclone separator and can be due to a larger number of guide vanes ($i_k = 5$) than usually used in the cyclone separators in the air filters of motor vehicles ($i_k = 4$).

The ratio of the diameter D_w of the inlet port to the diameter of the outlet duct d_w is determined by the following parameter:

$$k_d = \frac{D_w}{d_w}. \tag{15}$$

In the existing design, the value is $k_d = 2$, which is considered the optimum value [21, 32, 56].

In case of the tested cyclone, the parameter is:

$$k_d = \frac{D_w}{d_w} = \frac{66}{19} = 3.47.$$

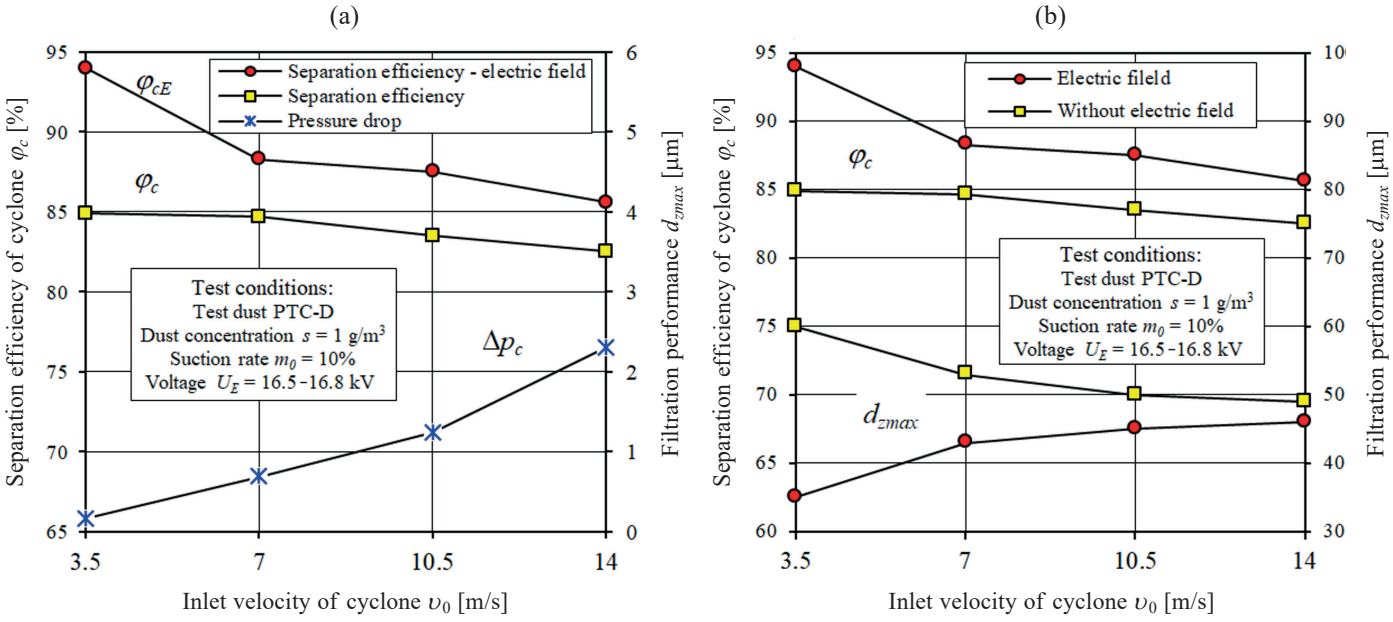

Fig. 10. Performance characteristics of the vortex tube separator with and without electric field depending on the inlet velocity of cyclone υ_0: a) separation efficiency $\varphi_c = f(\upsilon_0)$ i pressure drop $\Delta p_c = f(\upsilon_0)$, b) separation efficiency $\varphi_c = f(\upsilon_0)$ and filtration performance $d_{zmax} = f(\upsilon_0)$

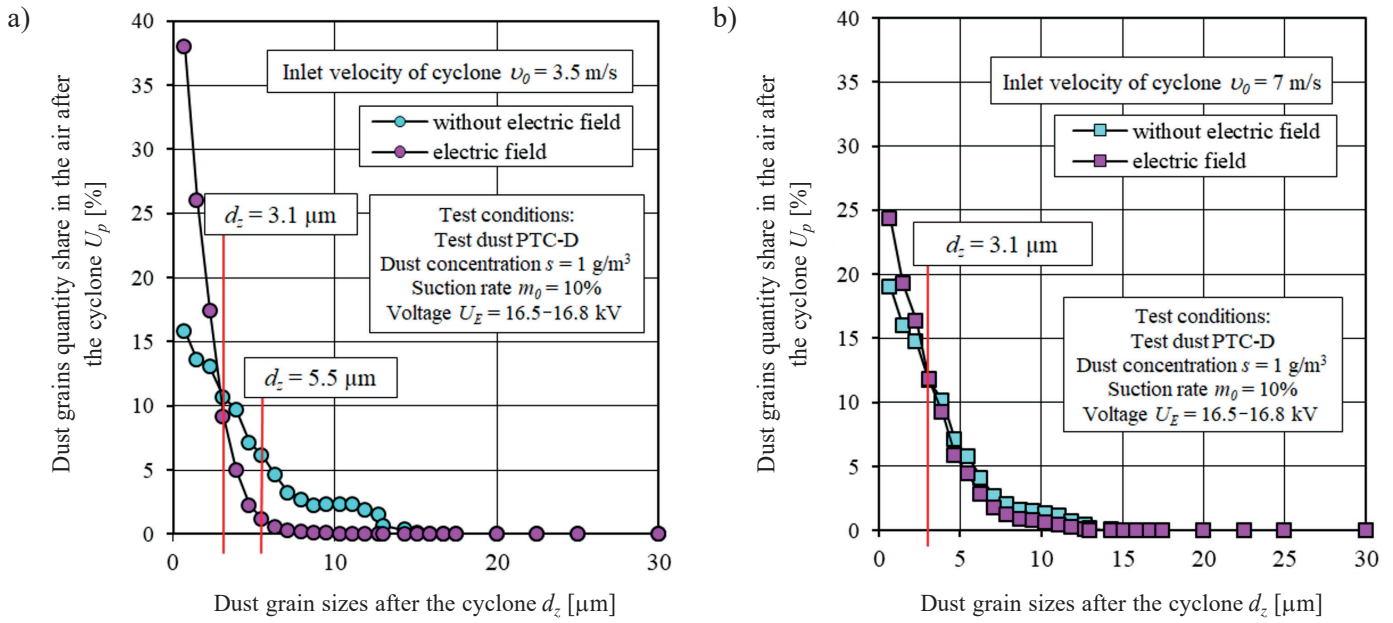

Fig. 11. The percentage share of dust particles in the air downstream of the vortex tube separator with and without electric field at a) $\upsilon_0 = 3.5$ m/s, and b) $\upsilon_0 = 7$ m/s

The cyclones for which k_d is higher than the optimum value are characterized by high pressure drop, as is the case with the tested cyclone separator, however, they can achieve better separation efficiency.

With an increase in air flow rate Q_G through the tested cyclone separator, and thus the inlet velocity of cyclone υ_0, the separation efficiency of the cyclone separator without electric fields decreases: at $\upsilon_0 = 3.5$ m/s to $\varphi_c = 84.9\%$, and at $\upsilon_0 = 14$ m/s to $\varphi_c = 82.5\%$ (Fig. 10b).

As a result of the electric field, a significant increase in separation efficiency is observed, in particular at low inlet velocity of cyclone. At $\upsilon_0 = 3.5$ m/s, the separation efficiency φ_c increased to $\varphi_c = 93.9\%$, i.e. by 10%. At higher inlet velocity of cyclone, the increase in separation efficiency of the cyclone separator, depending on the electric field is low (between 3 and 4%) and at $\upsilon_0 = 14$ m/s is $\varphi_c = 85.6\%$.

An increase in inlet velocity of cyclone υ_0 at $\upsilon_0 = 3.5$ to 14 m/s will result in a slight increase in the maximum diame-

ter of the dust particles d_{zmax} in the air filtered by the cyclone separator without electric field. At inlet velocity of cyclone $\upsilon_0 = 3.5$ m/s it is $d_{zmax} = 60$ µm, and at $\upsilon_0 = 14$ m/s it is slightly lower at $d_{zmax} = 50$ µm (Fig. 10b). Large size of the dust particles may be due to excessive pitch of the swirl vane blades. For the cyclone with electric field, the dust particles d_{zmax} are significantly smaller – at $\upsilon_0 = 3{,}5$ m/s the maximum particle size is $d_{zmax} = 35$ µm.

Here we can see a clearly differentiated (inverse) effect of inlet speed on d_{zmax} with and without electric field. However, as the inlet velocity υ_0 increases, this phenomenon disappears, because dust grain maximum diameter values d_{zmax} have increasing values for $\upsilon_0 = 14$ m/s – $d_{zmax} = 45$ µm. Large dust grains presence in the exhaust air has an impact on filtration efficiency, which, as the inlet speed υ_0 increases, their value decreases (Fig. 10b). For higher inlet velocities, dust grain diameters d_{zmax} have increasing values and for $\upsilon_0 = 14$ m/s it is $d_{zmax} = 45$ µm. The analysis shows that the impact of the electric field on dust grains found in the cyclone rotating air stream decreases with the increase of inlet speed υ_0. This is due to the shorter particles residence time in the cyclone electric field. Fig. 11 shows the test and calculation results of the percentage share U_p of dust particles in the air downstream of the cyclone with and without electric field at two different inlet velocity of cyclone $\upsilon_0 = 3.5$ m/s and $\upsilon_0 = 7$ m/s.

At constant inlet velocity of cyclone υ_0, constant air flow rate Q_G and extraction rate m_0 and similar filter condition (with or without electric field), a systematic decrease in the number of dust particles in the air downstream of the cyclone can be observed, validating the theory of cyclone separator operation. The percentage share U_p for each measuring interval Δd_z decreases until reaching a minimum value U_{pmin} – a percentage share of a single dust particle with a maximum size of d_{zmax} in a total number of dust particles N.

Supplying the electric field at $U_E = 16.5$ to 16.8 kV results in the percentage share U_p of dust particles with diameters over $d_z = 3.1$ µm to decrease during the same measuring intervals, and of dust particles with the diameter below this value to increase, although the effect is slower at lower flow rates. At inlet velocity of cyclone of $\upsilon_0 = 3.5$ m/s the effect of electric field resulted in a decrease in percentage share of dust particle with a size $d_z = 5.5$ µm from $U_p = 6.12\%$ to $U_p = 1.16\%$ and simultaneous increase in percentage share of dust particles with $d_z = 0.7$ µm from $U_p = 15.8\%$ to $U_p = 38.0\%$ (Fig. 11). At inlet velocity of cyclone of $\upsilon_0 = 7$ m/s, the effect of electric field on the separation efficiency is insignificant.

The effect of electric field ($U_E = 16.5$ to 16.8 kV) on the separation efficiency of the tested cyclone separator can be observed at lower inlet velocity of cyclone and applies to the dust particles over 2.3 to 3.1 µm (Fig. 12).

6. Vortex tube separator – variant W2 – test result analysis

The second stage of the tests covered a vortex tube separator (variant W2), with a design modified compared to the cyclone separator tested in the first stage, based on the test results and observations from the first stage of tests (Fig. 14).

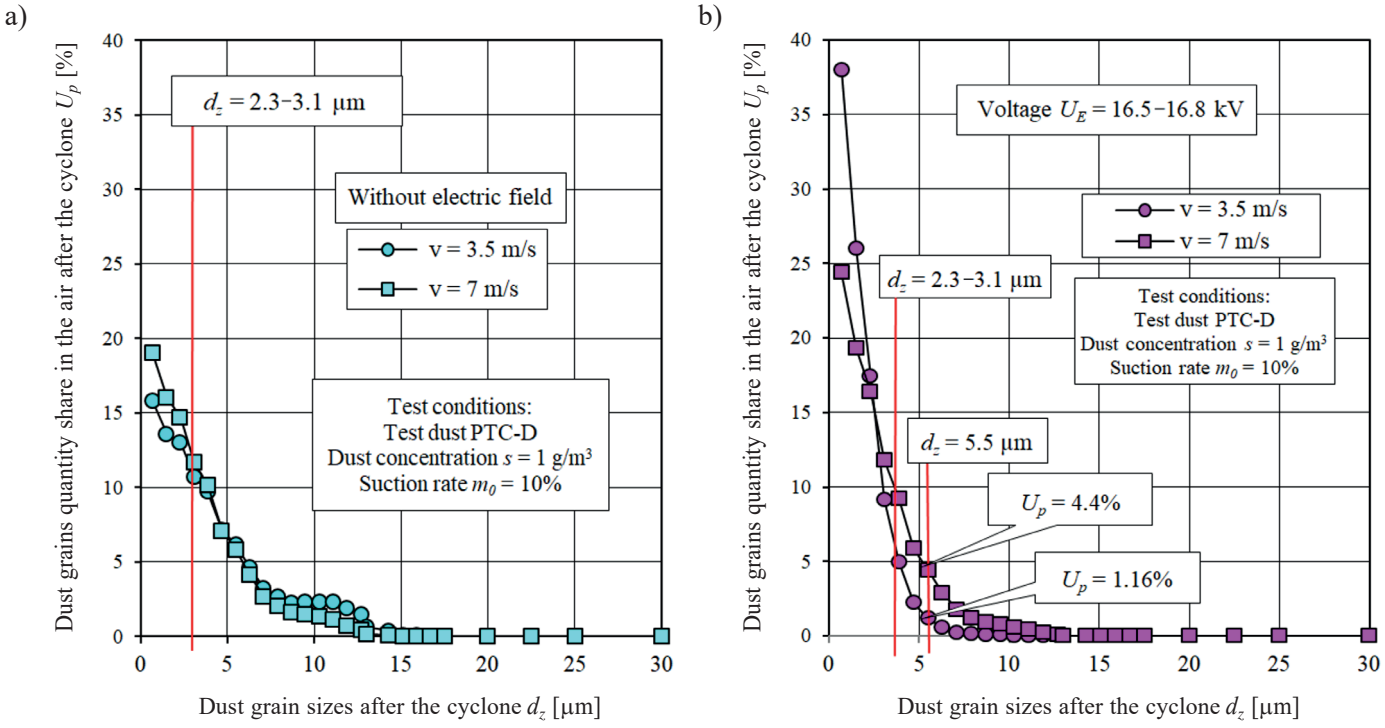

Fig. 12. The percentage of dust particles in the air downstream of the vortex tube separator at $\upsilon_0 = 3.5$ m/s, and $\upsilon_0 = 7$ m/s: a) without electric field, b) with electric field

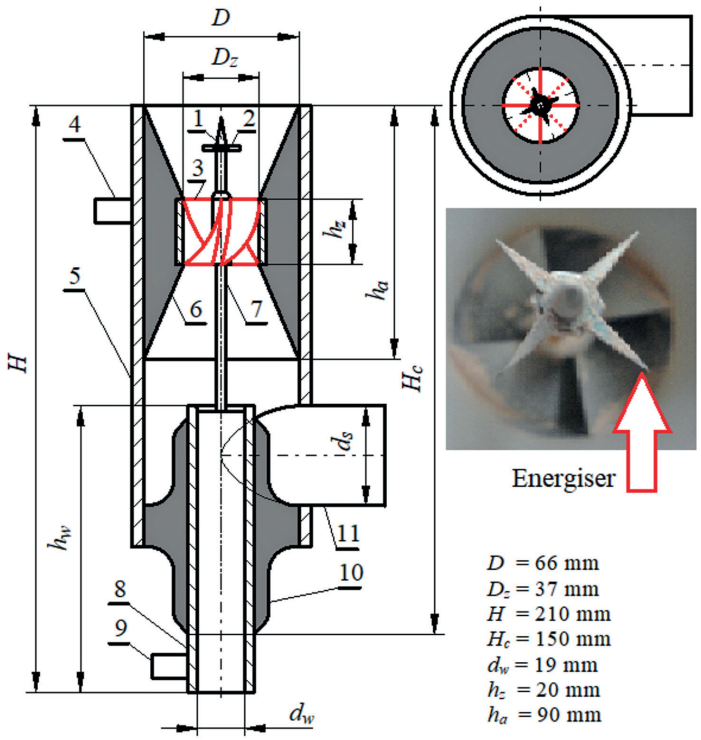

Fig. 13. Diagram of the vortex tube separator – variant W2: 1 – negative electrode tip, 2 – energiser, 3 – swirl vane, 4 – high voltage terminal (ground), 5 – cylindrical section of the cyclone (housing-ground), 6 – top insulator, 7 – connecting pin, 8 – outlet line, 9 – high voltage terminal (negative), 10 – bottom insulator, 11 – dust extraction line [64]

The modifications of W2 cyclone separator included:

1. A 4-blade swirl vane with lower pitch used instead of a 5-blade swirl vane to generate the air flow. Each blade has an angle of 135° with 45° overlap.
2. A special "energiser" increasing the current leakage installed at the tip of the negative electrode (at the cyclone separator inlet).
3. Reduced pitch of the swirl vane blades ($S = 53{,}3$ mm).
4. Modified aerosol inlet to the cyclone separator to achieve better aerodynamics.
5. Extra insulation layer on the outlet tube to increase the voltage to $U_E = 18.5$ to 19.0 kV.

The second stage of the test included measurement of the same performance characteristics of the vortex tube separator (W2) under the same test conditions at different inlet velocity of cyclone ($\upsilon_0 = 1.75 \div 7$ m/s). As a result of cyclone testing in the W1 version, a systematic decrease in filtration efficiency above the inlet speed $\upsilon_0 = 7$ m/s was obtained – for a cyclone with an electric field like without an electric field, hence the decision to put W2 cyclone testing range towards lower inlet speeds. Figure 14 and 15 show the performance test results of the vortex tube separator (with and without electric field).

Vortex tube separator (version W2) during tests without electric field is characterized by much greater efficiency φ_c and filtration accuracy (smaller maximum values of dust grains $d_{z\,max}$) in the range $\upsilon_0 = 1.75$–7.0 m/s than the cyclone in version W1. Obtained effect of increasing efficiency and cyclone filtration accuracy (W2) is a result of using a swirler with altered blade geometry. Each of the blades covers an angle of 135°, which gives a covering of 45°. This prevents particles free flow through the swirler without contact with the blade surface. In addition, the blades have a smaller pitch ($S = 53.3$ mm), which ensures more intense turbulence.

A significant increase in the separation efficiency was observed due to the electric field (W2), in particular at low inlet velocity of cyclone. At $\upsilon_0 = 1.75$ m/s, the separation efficiency φ_c increased from $\varphi_c = 88.7\%$ to $\varphi_c = 96.3\%$, by 8.5% – Fig. 14. At higher inlet velocity of cyclone, an increase in separation efficiency due to the electric field is insignificant (no more than 3%) and at $\upsilon_0 = 7$ m/s is $\varphi_c = 86.8\%$.

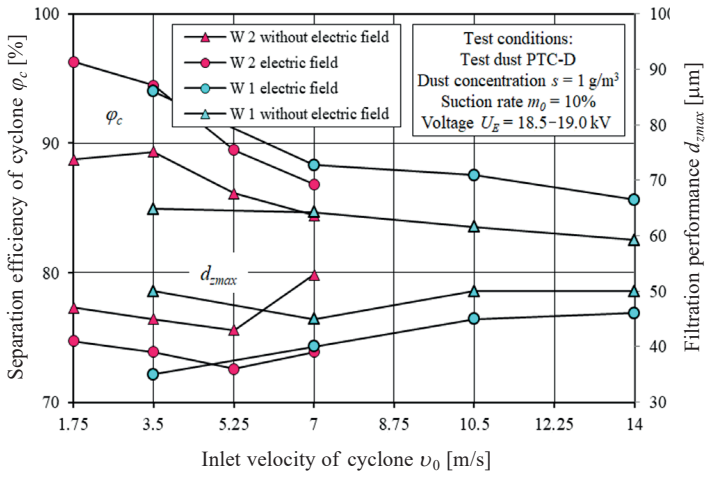

Fig. 14. Separation efficiency $\varphi_c = f(\upsilon_0)$ and filtration performance $d_{z\,max} = f(\upsilon_0)$ as a function of inlet velocity of cyclone of the υ_0 vortex tube separator (W1 and W2) with and without electric field

W2 cyclone efficiency increase is caused by the use of an electric field resulting from the same level voltage ($U = 18.5$ kV) is at the level obtained for cyclone W1 tested in the same conditions (Fig. 14).

With an increase in air stream Q_G flowing through the cyclone, and thus the inlet velocity of cyclone υ_0, the separation efficiency without electric field is between $\varphi_{c2} = 88.7$ to 84.8%, and reaches its maximum $\varphi_{cmax} = 89.3\%$ at 3.5 m/s – Fig. 14. The separation efficiency φ_c of the cyclone without electric field (W2) is over 5% higher than tested for W1 cyclone under the same conditions.

An increase in inlet velocity of cyclone between $\upsilon_0 = 1.75$ to 5.25 m/s results in a slight increase in filtration performance of the cyclone separator (decrease in maximum dust particle size $d_{z\,max}$) both with and without electric field. An increase in inlet velocity of cyclone over $\upsilon_0 = 5.25$ m/s results in a decrease in filtration performance. The air filtered by the cyclone separator without electric field contains dust particles with $d_{z\,max} = 47$ to 53 μm. For the cyclone with electric field, the maximum dust particle diameters $d_{z\,max}$ are slightly smaller. At inlet velocity of cyclone $\upsilon_0 = 1.75$ m/s the maximum dust particle diameter is $d_{z\,max} = 40$ μm, and at $\upsilon_0 = 5.25$ m/s – $d_{z\,max} = 35$ μm.

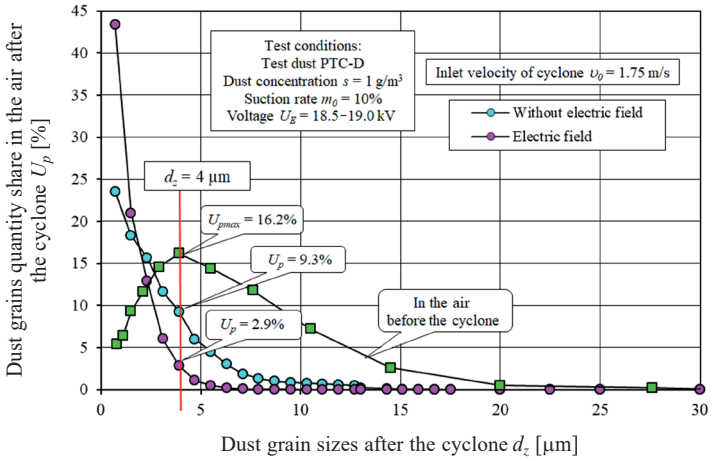

Fig. 15. Dust grains quantity share in the air after and before the vortex tube separator (W1 and W2) with and without electric field U_p [%]

Figure 15 shows the comparative analysis of particle size distribution of dust in the air upstream and downstream of the cyclone separator at the inlet velocity of cyclone of $\upsilon_0 = 1.75$ m/s with and without electric field.

In a total number of test dust particles in the air upstream of the cyclone, the dust particle with $d_z = 4$ µm have the highest share – $U_{pmax} = 16.2\%$. Percentage share of dust particles in filtered air (downstream of the cyclone) decreases hyperbolically for higher dust particle diameters d_z from $d_z = 0.7$ µm. For the cyclone with electric field, percentage share of dust particles in filtered air are significantly lower than for the cyclone without electric field. For example, for the cyclone without electric field, the percentage of dust particles with $d_z = 4$ µm is $U_p = 9.3\%$, whereas for the cyclone with electric field, the percentage is $U_p = 2.9\%$.

In the tested cyclone, the best separation efficiency was observed for the dust particles with $d_z = 3$ to 20 µm. According to [7, 10, 11, 15], the highest wear of the mating machine parts is caused by the dust particles with a diameter of $d_z = 1$ to 35 µm.

7. Summary and conclusions

The purpose of the study was to evaluate the design of a vortex tube separator regarding its separation efficiency with and without electric field generated within the area of swirling aerosol. The measurements of the separation efficiency $\varphi_c = f(\upsilon_0)$ and filtration performance $d_{zmax} = f(\upsilon_0)$ and pressure drop $\Delta p_c = f(\upsilon_0)$ led to the following conclusions:

1. The electric field generated in the area of swirling aerosol flow rate in the cyclone separator resulted in an increase in separation efficiency within the entire range of the tested inlet velocity of cyclone from 1.75 m/s to 14 m/s. However, an increase in separation efficiency at the inlet velocity of cyclone from 1.75 m/s to 3.5 m/s is significantly higher (up to 96%) compared to other flow rates and is over 12%, which might indicate practical applicability of the tested solutions. At other flow rates, the increase does not exceed 3 to 4% and at $\upsilon_0 = 14$ m/s the separation efficiency is $\varphi_{cp} = 85.62\%$, indicating that the electric field is more effective (longer effect) in relation to the dust particles moving at lower velocities.
2. The electric field in the area of swirling aerosol in the vortex tube separator results in an increase in filtration performance, however, the increase is slight. The maximum size of dust particles d_{zmax} in the air downstream of the cyclone (at inlet velocity of cyclone $\upsilon_0 = 1.75$ to 7 m/s) is $d_{zmax} = 43$ to 53 mm without electric field and $d_{zmax} = 36$ to 41 mm with electric field. The effect of the electric field on dust particles is higher at lower air flow rates.
3. With an increase in dust particle size, the percentage share (for the same measuring intervals) in the filtered air downstream of the filter decreases, validating the theory of cyclone separator operation, however, the effect of the electric field decreases the percentage share of dust particles over $d_z = 2.3$ to 3.5 mm and increases the percentage of dust particles below this range, suggesting that the effect of the electric field in the cyclone separator is higher on particles larger than approx. 3 mm.
4. Cyclone presented in the work can be used in many ways: in industry and in automotive technology, as an element of several or several dozen cyclones – called a multicyclone. Multicyclone can be used as first stage of inlet air filtration in combustion engines. A set of several cyclones can be used as a filter in the exhaust suction device from a welding station or iron foundry.

Further studies aimed at improving the cyclone separator operation with the electric field should be focused on:

1. Using higher electric field value, increasing the insulation thickness and increasing the cyclone dimensions.
2. Modifying the cyclone separator design:
   a) selecting the optimum cyclone length H based on the required efficiency;
   b) replacing the end of the cylindrical outlet tube with a cone with an inlet port diameter d_{w1} lower than d_w;
   c) changing the method of attaching the pin connecting the outlet tube with the swirl vane and removing the crosspiece at the outlet tube port.

References

[1] J. Warych, *The cleaning of gases: processes and equipment*, WNT Warsaw, 1998 (in Polish).
[2] Dust protection device Pall Centrisep® for helicopters type Mi-17/Mi-8MT, including various modifications, [Online] Available: http://www.pall.com/pdfs/Aerospace-Defense-Marine/AEMI17SRU.pdf. [in Russian]
[3] [Online] Available: http://www.pall.com/main/aerospace-defense-marine/products.page?pt=Cleaners&tab=1.
[4] AS332/EC725 Super Puma/Cougar Helicopter PUREair System, Data Sheet, [Online] Available: http://www.pall.com/pdfs/Aerospace-Defense-Marine/AEAS332EN.pdf.
[5] Cummins Direct Flow by Fleetguard, [Online] Available: www.cumminsfiltration.com.

[6] T. Dziubak, "The assessment of the possibilities of improvement of the extraction evenness, in multicyclone dedusters fitted in special vehicles", *Combustion Engines*. 4(151), 34–42 (2012).
[7] T. Dziubak, "Inlet air filtration in internal combustion engines", Military University of Technology. Warsaw, 2012.
[8] T. Grafe, M. Gogins, M. Barris, J. Schaefer, and R. Canepa, "Nanofibers in Filtration Applications in Transportation". *Filtration 2001 International Conference and Exposition*, Chicago, USA, 2001.
[9] MANN+HUMMEL PicoFlex®. The new compact air cleaner for your highest requirements. [Online] Available: www.mann-hummel.com.
[10] Cenrtisep Air Cleaner. PALL Corporation, USA 2004.
[11] T. Dziubak, "The effects of dust extraction on multi-cyclone and non-woven fabric panel filter performance in the air filters used in special vehicles", *Eksploatacja i Niezawodnosc – Maintenance and Reliability* 18(3), 348–357 (2016).
[12] T. Dziubak, "Modification of returnable cyclone with a tangent inlet construction", *Bulletin of the Military University of Technology. Warsaw*, 55(2), 279–301 (2006).
[13] T. Dziubak, "The problems of the air filtration in the vehicle engines exploitated in large pollution conditions", *ZEM Polish Academy of Sciences* 4(124), 181–197 (2000).
[14] T. Dziubak, "Experimental research of axial cyclones of combustion engines air filters", *Bulletin of the Military University of Technology, Warsaw* 62(2), 201–217 (2013).
[15] T. Jaroszczyk and T. Ptak, "Experimental Study of Aerosol Separation Using a Minicyclone", *10th Annual Powder and Bulk Solids Conference*. USA, 1985.
[16] B. Karwat, R. Machnik, J. Niedźwiedzki, and M. Nogaj, "Selecting operating parameters of an electrostatic precipitator decreasing emission of solid fuels fly ashes", *Eksploatacja i Niezawodnosc – Maintenance and Reliability* 20(3), 495–501 (2018).
[17] B. Karwat, M. Nocuń, R. Machnik, and J. Niedźwiedzki, "Modelling and study the effect of selected design features for the operating parameters of industrial electrostatic precipitators", *Eksploatacja i Niezawodnosc – Maintenance and Reliability* 18(3), 325–332 (2016).
[18] R. Machnik, B. Karwat, M. Nocuń, and J. Niedźwiedzki, „Wpływ fizykochemicznych właściwości popiołów lotnych ze spalania węgli na proces elektrostatycznego odpylania spalin", *Przemysł Chemiczny* 94(9), 1530–1533 (2015).
[19] W. Matysiak, T. Tański, and M. Zaborowska, "Manufacturing process and characterization of electrospun PVP/ZnO NPs nanofibers", *Bull. Pol. Ac.: Tech*. 67(2), 193–200 (2019).
[20] A.-M. Azad, M. Noibi, and M. Ramachandran, "Fabrication and characterization of 1-D alumina (Al_2O_3) nanofibers in an electric field", *Bull. Pol. Ac.: Tech*. 55(2), 195–201 (2007).
[21] A. Haider. S. Haider, and I-K. Kang, "A comprehensive review summarizing the effect of electrospinning parameters and potential applications of nanofibers in biomedical and biotechnology", *Arabian J. Chem*. 11, 1165–1188 (2018).
[22] T.A. Kowalewski, S. Blonski, and S. Barral, "Experiments and modeling of electrospinning process", *Bull. Pol. Ac.: Tech*. 53(4), 385–394 (2005).
[23] N. Bojdo and A. Filippone, "A comparative study of helicopter engine air particle separation technologies". The University of Manchester, 2012.
[24] J. Wang, S.C. Kim, and D.Y.H. Pui, "Figure of Merit of Composite Filters with Micrometer and Nanometer Fibers", *Aerosol Sci. Technol*. 42, 722–728 (2008).
[25] M. Wasilewski and L.S. Brar, "Effect of the inlet duct angle on the performance of cyclone separators", *Sep. Purif. Technol*. 213, 19–33 (2019).
[26] H. Zhou, Z. Hu, Q. Zhang, Q. Wang, and X. Lv, "Numerical study on gas-solid flow characteristics of ultra-light particles in a cyclone separator", *Powder Technol*. 344, 784–796 (2019).
[27] O.R. Nassaj, D. Toghraie, and M. Afrand, "Effects of multi inlet guide channels on the performance of a cyclone separator", *Powder Technol.* 356, 353–372 (2019).
[28] B. Zhao and Y. Su, "Particle size cut performance of aerodynamic cyclone separators: Generalized modeling and characterization by correlating global cyclone dimensions", *J. Aerosol Sci.* 120, 1–11, (2018).
[29] K. Elsayed, "Optimization of the cyclone separator geometry for minimum pressure drop using Co-Kriging", *Powder Technol*. 269, 409–424 (2015).
[30] K.W. Chu, B. Wang, D.L. Xu, Y.X. Chen, and A.B. Yu, "CFD–DEM simulation of the gas–solid flow in a cyclone separator", *Chem. Eng. Sci*. 66(5), 834–847 (2011).
[31] T. Dziubak, L. Bąkała, M. Karczewski, and M. Tomaszewski, "Numerical research on vortex tube separator for special vehicle engine inlet air filter", *Sep. Purif. Technol*. 237, 116463 (2020)
[32] N. Bojdo and A. Filippone, "A Simple Model to Assess the Role of Dust Composition and Size on Deposition in Rotorcraft Engines", *Aerospace* 6(44), 1–26 (2019).
[33] A. Filippone and N. Bojdo, "Turboshaft engine air particle separation", *Prog. Aerosp. Sci*. 46, 224–245 (2010).
[34] C.J. Tsai, S.C. Chen, R. Przekop, and A. Moskal, "Study of an Axial Flow Cyclone to Remove Nanoparticles in Vacuum", *Environ. Sci. Technol*. 41, 1689–1695 (2007).
[35] P.A. Funk, G.A. Holt, and D.P. Whitelock, "Novel cyclone empirical pressure drop and emissions with heterogeneous particulate", *J. Aerosol Sci*. 74, 26–35 (2014).
[36] Z. Ji, Z. Xiong, X. Wu, H. Chen, and H. Wu, "Experimental investigations on a cyclone separator performance at an extremely low particle concentration", *Powder Technol.* 191, 254–259 (2009).
[37] Y. Jo, Ch. Tien, and M.B. Ray, "Development of a post cyclone to improve the efficiency of reverse flow cyclones", *Powder Technol*. 113, 97–108 (2000).
[38] H.T. Kim, Y. Zhu, W.C. Hinds, and K.W. Lee, "Experimental study of small virtual cyclones as particle concentrators", *J. Aerosol Sci*. 5(33), 721–733 (2002).
[39] K.S. Lim, H.S. Kim, and K.W. Lee, "Characteristics of the collection effciency for a cyclone with different vortex finder shapes", *J. Aerosol Sci*. 6, 743–754 (2004).
[40] G.B. Sakura and A.Y.T. Leung, "Experimental Study of Particle Collection Efficiency of Cylindrical Inlet Type Cyclone Separator", *Int. J. Environ. Sci. Develop.* 3, 160–164 (2015).
[41] T. Dziubak, "Performance characteristics of air intake pleated panel filters for internal combustion engines in a two-stage configuration", *Aerosol Sci. Technol*. 52(11), 1293–1307 (2018).
[42] T. Dziubak and S. Szwedkowicz, "Operating properties of non-woven fabric panel filters for internal combustion engine inlet air in single and two-stage filtration systems", *Eksploatacja i Niezawodnosc – Maintenance and Reliability* 17(4), 519–527 (2015).
[43] A.G. Titov, "The Impact of re-entrainment on the electrocyclone effectiveness", *Sep. Purif. Technol*. 156, 795–802 (2015).
[44] J. Li and W. Cai, "Study of cut diameter of solid-gas separation in cyclone with electrostatic excitation", *J. Electrostat*. 60, 15–23 (2004).

[45] J. Li and W. Cai, "Theory and Application of cyclone with impulse electrostatic excitation for cleaning molecular gas", *J. Electrostat*. 64, 254–258 (2006).
[46] V.S. Aslamova, M.I. Arshinskii, N.A. Bragin, and A.A. Zhabei, "Study of a direct-flow cyclone with intermediate dust collection", *Chem. Pet. Eng.* 45, 372–375 (2009).
[47] G.Y. Lin, L.T. Cuc, W. Lu, C.J. Tsai H.M. Chein, and F.T. Chang, "High-efficiency wet electrocyclone for removing fine and nano sized particles", *Sep. Purif. Technol*. 114, 99–107 (2013).
[48] J.P. Zhang, Z.T. Zha, P. Che, W.G. Pan, D.M. Hu, and F.Q. Li, "Theoretical study on submicron particle escape reduced by magnetic. confinement effect in low inlet speed electrostatic cyclone precipitators", *Powder Technol*. 339, 1005–1011 (2018).
[49] L. Horne, "Electro cyclone technology: A media-free option for engine cleaning?", *Filtr. Sep*. 2, 12–15 (2006).
[50] A.G. Titov, Z.R. Gil'vanova, N.V. Inyushkin, S.A. Ermakov, I.P. Shchelchkov, A.I. Aitova, M.G. Man'kov, N.A. Tokareva, and S.A. Perfilov, "Efficiency of Electrostatic Cyclone Operation", *Chem. Pet. Eng*. 49, 655–659 (2014).
[51] H. Yoshida, K. Fukui, W. Pratarn, and W. Tanthapanichakoon, "Particle separation performance by use of electrical hydro-cyclone", *Sep. Purif. Technol.* 50, 330–335 (2006).
[52] C.J. Chen, "Enhanced collection efficiency for cyclone by applying an external electric field", *Sep. Sci. Technol*. 36, 499–511 (2001).
[53] P.W. Dietz, "Electrostatically enhanced cyclone separators", *Powder Technol*. 31, 211–216 (1982).
[54] J. Pluciński, L. Gradoń, and J. Nowicki, "Collection of aerosol particles in a cyclone with an external electric field", *J. Aerosol Sci*. 20(6), 695–700 (1989).
[55] L. Gradoń, H. Luckner, A. Podgórski, and Z. Wertejuk, "Separation of neutral and charged aerosol particles in cyclones with external electric field", *J. Aerosol Sci.* 29, 927–928 (1998).
[56] H. Amjadsoroudi, F.G. Shahna, A. Bahrami, and J. Fardmal, "Assessing Electrocyclone Performance in Collecting Smaller, than 1 μm Silica Airborne Particles", *Iran. J. Health Environ*. 6, 45–53 (2013).
[57] R.R. Boericke, W.G. Giles, P.W. Dietz, G.A. Kallio, and J.T. Kuo, "Electrocyclone for High-Temperature, High-Pressure Dust Removal", *J. Energy*. 1, 43–49 (1983).
[58] L. Gradoń, H. Luckner, A. Podgorski, and Z. Werterjuk, "Separation of neutral and charged aerosol particles in cyclones with external electric field", *J. Aerosol Sci*. 29, 927–928 (1998).
[59] P. Kabsch, *Dust extraction and dust collectors*, WNT, Warsaw 1992 (in Polish).
[60] K.S. Lim, H.S. Kim, and K.W. Lee, "Comparative performances of conventional cyclones and a double cyclone with and without an electric field", *J. Aerosol Sci*. 35, 103–116 (2004).
[61] K.S. Lim, K.W. Lee, and M.R Kuhlman, "An Experimental Study of the Performance Factors Affecting Particle Collection Efficiency of the Electrocyclone", *Aerosol Sci. Technol*. 35, 969–977 (2001).
[62] J.S. Shrimpton and R.I. Crane, "Small electrocyclone performance", *Chem. Eng.Technol*. 24, 951–955 (2001).
[63] A. Jaworek, A. Krupa, and T. Czech, "Modern electrostatic devices and methods for exhaust gas cleaning: a brief review", *J. Electrostat*. 65, 133–155 (2007).
[64] T. Dziubak, Report from the research work. No PBN/03–453/2016/WAT „Prototype vortex tube separator tests". Order, LASER-STAR Sp. z o.o. Sp. k. Toruń. WAT Warsaw, 2016.